

UDK: 678.7; 553.612; 621.746.6

The Effect of the Concentration of Alkaline Activator and Aging Time on the Structure of Metakaolin Based Geopolymer

Marija Ivanović^{1*}, Ljiljana Kljajević¹, Jelena Gulicovski¹, Marijana Petkovic², Ivona Jankovic-Castvan³, Dušan Bučevac¹, Snežana Nenadović¹

¹Laboratory for Materials Science, Institute for Nuclear Sciences Vinča, University of Belgrade, Belgrade, Serbia

²CQM-Madeira Chemistry Research Centre, University of Madeira, Funchal, Portugal

³Faculty of Technology and Metallurgy, University of Belgrade, Belgrade, Serbia

Abstract:

This paper outlines the production of an inorganic polymer/geopolymer using a metakaolin by an environmental friendly, energy saving, clean technology to conserve natural environment and resources. The influence of alkali activation, i.e. different concentration of NaOH as a component of alkali activator mixture on the process of geopolymerization of metakaolin is investigated. Also, process of aging time of geopolymer is followed by several analytical methods. The structure of metakaolin and metakaolin based geopolymers and their physicochemical properties were studied using X-ray diffraction (XRD), Fourier transformation infrared spectroscopy (FTIR) and after 28days scanning electron microscopy (SEM) with energy dispersive spectroscopy (EDS) was applied for the surface characterization of the samples. A shift of the Si-O or Si-O-X (X=Al, Si, Na...) bands as the molarity of activator increasing during geopolymerization process was observed by FTIR. Mass spectra of geopolymers were characterized by MALDI TOF mass spectrometer. Structural reorganization of geopolymer samples occurs during the curing/aging in accordance with a geopolymerization mechanism.

Keywords: Metakaolin; Alkali activation; Inorganic polymer; Aging time; MALDI TOFMS.

1. Introduction

Geopolymers are innovative class of ceramic materials that possess advanced technological features, such as low energy consumption of production for construction purposes. Geopolymers are usually obtained through inexpensive and ecofriendly synthetic procedures with low waste gas emission [1-4], which is one of the reasons why they are called the “green materials” [5].

Synthesis of geopolymers can be made by mixing a reactive aluminosilicate material with high alkaline solutions. NaOH or KOH are the most commonly used components of activator solutions. Most of the research and knowledge [6] concerning a mechanism of geopolymerization are based on the use of metakaolin as a precursor. Metakaolin is a good source of silicon and aluminum which are highly reactive and react with alkaline activator.

The concentration of hydroxide in the solution of activator plays an important role in the process of geopolymerization [7]. Studies of the effect of hydroxide led to important

*) Corresponding author: marija.ivanovic777@gmail.com

discoveries about the mechanism of the reaction. If working with highly concentrated hydroxide solution (10 mol/dm^3 and more), the pH will be sufficiently high to reach the dissolution of silicon from the raw material as well as to prevent the dissolution of the $\text{Ca}(\text{OH})_2$ [8].

Besides the pH of alkali activator solutions, temperature of geopolymerization and duration of geopolymerization are important parameters of the process. In a work of Jaarsveld and coworkers [9], the samples were at an elevated temperature usually retained 12 or 24 hours, and during the first phase of the reaction the water was consumed. This water consumed in the hydrolysis and dissolution of the initial species in the raw material will be ejected from the geopolymers matrix with further reaction to take a place [9]. Looking at the overall reaction can be concluded that water is a reaction medium as such it is not necessary for the reaction of geopolymerization. In addition to condensation, release of water comes in the later stages of the reaction, as well as during aging [10]. In our previous research were concluded, that after activation of metakaolin, the geopolymeric gel was formed which suggesting that the structure experiences growth [11].

The presented study aims at analyzing the effect of different concentrations of sodium hydroxide (NaOH) on the structure of obtained inorganic polymer during the geopolymerization reaction. The physical and chemical properties from the starting material to the final geopolymers have been monitored to understand the geopolymerization mechanism.

2. Materials and Experimental Procedures

Metakaolin (MK) was prepared by calcining kaolinite at $750 \text{ }^\circ\text{C}$ for one hour and the physicochemical properties of kaolin obtained from Rudovci (Lazarevac - Serbia) were presented in our previous work [12]. Tab. I shows the chemical composition of MK. The elemental composition analysis was conducted by XRF (type UPA XRF 200) and modified forms expressed as weight percentages of metal oxides.

Tab. I The chemical composition of MK.

MK	SiO_2	Al_2O_3	Fe_2O_3	MgO	CaO	Na_2O	K_2O	L.O.I.
(%wt)	55.03	35.44	4.39	1.25	1.38	/	2.07	

The alkaline activator solution was prepared from solution of Na_2SiO_3 (technical grade) supplied by manufacturer from Serbia, "DEM Company", Belgrade, (the chemical composition of Na_2SiO_3 was comprised of $\text{Na}_2\text{O} = 14.7\%$, $\text{SiO}_2 = 29.4\%$, and water 55.9% , mass ratio, and 2M, 4M, 6M and 8M NaOH (analytical grade) (volume ratio $\text{Na}_2\text{SiO}_3/\text{NaOH} = 1.6$);

Tab. II The molar ratio of $\text{SiO}_2/\text{Na}_2\text{O}$ and $\text{Al}_2\text{O}_3/\text{Na}_2\text{O}$ of GP2M, GP4M, GP6M and GP8M.

	GP2M	GP4M	GP6M	GP8M
$\text{SiO}_2/\text{Na}_2\text{O}$	3.50	2.85	2.55	2.45
$\text{Al}_2\text{O}_3/\text{Na}_2\text{O}$	1.98	1.58	1.48	1.46

The geopolymer (GP) samples were formed from metakaolin and the four different alkaline solution (solid/liquid ratio was 1:1), which were mixed for 10 min and then left at room temperature for one day. Finally, the sample mixture was kept in a drying oven for 2 days at $60 \text{ }^\circ\text{C}$. The curing and in the same time aging, of geopolymer samples has been followed for 7, 14, 21 and 28 days in covered molds at opened chamber and room relative humidity of 95.

Tab. II show the molar ratio of $\text{SiO}_2/\text{Na}_2\text{O}$ and $\text{Al}_2\text{O}_3/\text{Na}_2\text{O}$ of all obtained geopolymer samples geopolymer 2M sample -GP2M (a); geopolymer 4M sample -GP4M (b); geopolymer 6M sample- GP6M (c); geopolymer 8M sample- GP8M (d).

All samples were characterized by X-ray diffractometry (XRD) by using Ultima IV Rigaku diffractometer, equipped by Cu $K\alpha_{1,2}$ radiation, with a generator voltage of 40.0 kV and a generator current of 40.0 mA. The 2θ range of 5° - 80° was used for all powders in a continuous scan mode with a scanning step size of 0.02° at scan rate of $5^\circ/\text{min}$ using analog detector. For phase identification analysis was done using PDXL2 software (version 2.8.3.0) [13], with reference to ICDD database [14].

The functional groups of all considered samples were studied using FTIR spectroscopy. Samples were powdered finely and homogeneously dispersed in anhydrous potassium bromide (KBr) pellets (1.5/150 mg KBr). Spectra were taken at room temperature using a Bomem (Hartmann & Braun) MB-100 spectrometer set to give under formed spectra. The spectral data of the samples were collected in the 4000 - 400 cm^{-1} region.

Mass spectra of geopolymers were acquired at Autoflex Speed MALDI TOF mass spectrometer (Bruker, Bremen, Germany) equipped with pulsed smart beam TM-II laser. Emission wavelength of the laser was 355 nm and maximum repetition rate was 2 kHz. Samples were prepared by making a water suspension at concentration 10 mg/mL. Prior to application on the stainless steel MALDI target, samples were mixed with DHB solution in methanol (concentration 10 mg/mL) in a volume ratio 1:1. After vigorous mixing, a small volume (1 μL) was applied on the sample plate and left at room temperature to dry. Matrix for MALDI TOF MS, 2,5-dihydroxybenzoic acid (DHB), trifluoroacetic acid (TFA) and solvents for matrix-assisted laser desorption and ionization time-of-flight mass spectrometry were acquired from Sigma Aldrich (Germany).

The surface morphology of the samples was studied by field emission scanning electron microscopy (FESEM, Tescan MIRA 3 XMU) at 20 kV. The samples were sputter-coated with Au/Pd alloy before analysis.

3. Results and Discussion

The structural changes that occur during the geopolymerization of the alkali activated materials have been monitored as a function of the NaOH concentration (2-8M) and time (7, 14, 21 and 28 days) by FTIR and XRD methods.

The changes that have been characterized correspond to the second and third stages of the geopolymerization process [15]. Geopolimerization mechanism involves dissolving and hydrolysing aluminum and silicon in alkaline solution, transport and orientation of dissolved species accompanied by polycondensation and the creation of three-dimensional aluminosilicate networks [16]. The changes in XRD and FTIR spectrum indicate that there are fine changes of the aluminosilicates structure as the geopolymer synthesis progresses. Results show flexural strength, compressive strength and apparent density of the geopolymer increase along with the increase of concentration of NaOH solution within 4-12 mol/L.

3.1. Structural analysis

3.1.1. XRD analysis

Fig. 1 shows the XRD patterns of the geopolymers, GP2M (a); GP4M (b); GP6M (c); GP8M (d) cured at different curing times of 7, 14, 21 and 28 days (as indicated in the Fig.). One way to follow the crystalline structure changes during the geopolymerization reaction of the alkali activated materials is to compare the XRD patterns of the metakaolin and of the geopolymer cured at room temperature for 7 days, 14, 21 and 28 days then to

follow the changes of the XRD patterns of the samples cured for different times at room temperature. Finally, it is necessary to compare the XRD patterns of the samples cured at room temperature and different concentration NaOH. XRD analysis almost of all geopolymer samples revealed their amorphous-like structure with the position of an amorphous halo in the range 18° - 32° , which indicates short range ordering of the reference sample with crystalline admixture of SiO_2 (α -quartz, ICSD 89). The geopolymer shows the presence of the muscovite.

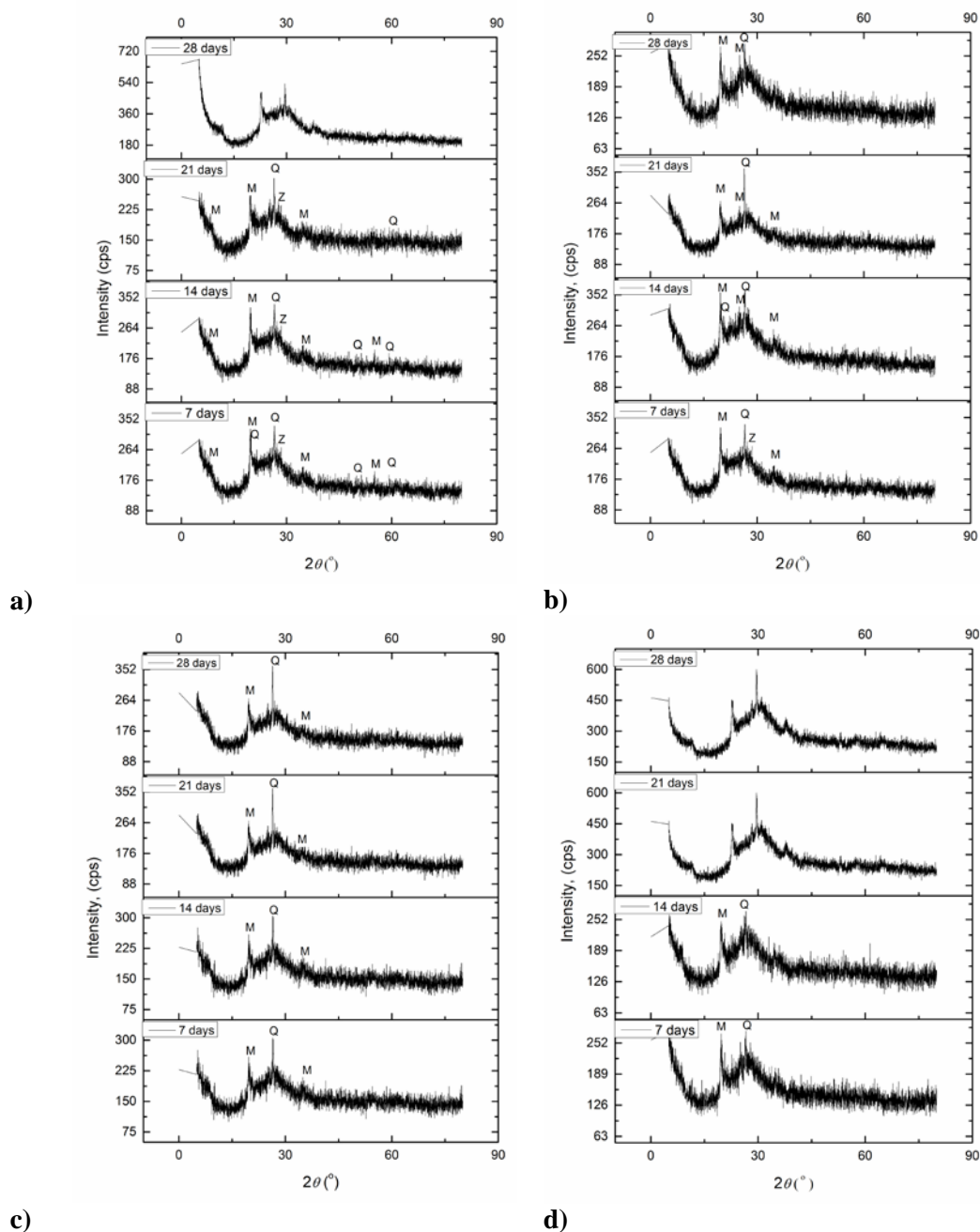


Fig 1. X-ray diffractograms of (a) GP2M sample (b) GP4M sample (c) GP6M sample (d) GP8M sample, every 7 days, until 28th day, as indicated in the diffractograms. The lines characteristic ascribed to quartz, muscovite, zeolite are marked in the diffractograms by letters Q, M, Z respectively.

When comparing the XRD patterns of the samples GP2M and GP4M aged at room temperature for 7, 14, 21 and 28 days that are shown in Fig. 1a and Fig 1b, it is observed that the intensity of the main peaks of quartz and muscovite after 28 days decrease. For GP6M and GP8M (Fig. 1c and Fig. 1d), there are no significant differences in the intensity of the identified crystalline phases. It is characteristic that amorphous halo is somewhat narrow and shifted to the higher angle for the GP8M which is aged for 21 and 28 days. Zhang et al. [17] found that proportion of the crystalline phase gradually increased at longer curing times. Furthermore, several authors [18-21] have noted the dissolution of the aluminosilicates from the raw materials and the recrystallization of new semi-crystalline phases at later stages of curing. The main difference with the current work is that we did not observe the appearance of new phases, for the time of monitoring.

3.1.2. FTIR analysis

Figs 2 and 3 shows the FTIR spectra of the geopolymers that have been aged for 7, 14, 21 and 28 days at room temperature: GP2M (Fig. 2a) and GP4M (Fig. 2b); GP6M (Fig. 3a) and GP8M (Fig. 3b). FTIR absorption spectra of these samples were compared to known absorption lines in literature. All spectra show a broad band with a maximum at $\sim 3450\text{ cm}^{-1}$ and a small band at 1635 cm^{-1} which are attributed to the stretching and deformation vibrations of the physically adsorbed water (O–H) molecules at the surface, respectively.

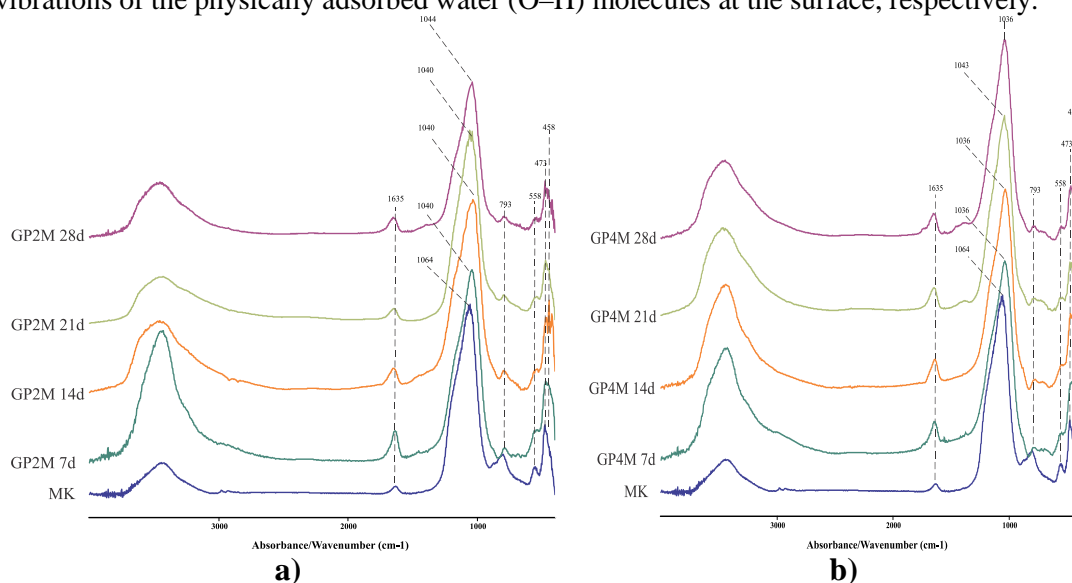


Fig. 2. FTIR of GP2M (a) and GP4M (b) samples after 7, 14, 21 and 28 days.

The FTIR spectra of all samples show a strong peak at $\sim 1000\text{ cm}^{-1}$ which is associated with Si–O–Si asymmetric stretching vibrations and is it the fingerprint of the geopolymerization [22]. In the spectral range of $1200\text{--}1000\text{ cm}^{-1}$ there are two broad bands, (Si–O–Si stretching vibration) and the second (Si–O and Si(Al)–O stretching vibration) [23, 24].

The effect of the NaOH concentration on the changes of the chemical structure that occur during the geopolymerization can be seen by comparing Fig. 2a and 2b and Fig. 3a and 3b. The bands located at 1100 and 1000 cm^{-1} that belong to the stretching of the Si–O bonds [25] shift to the right and the form of these bands change due to structural rearrangements of the geopolymer during 7-28 days of aging, and due to the effect of different concentrations of NaOH in the activator solutions. The broadening of these bands is more notorious using concentration 8M of NaOH.

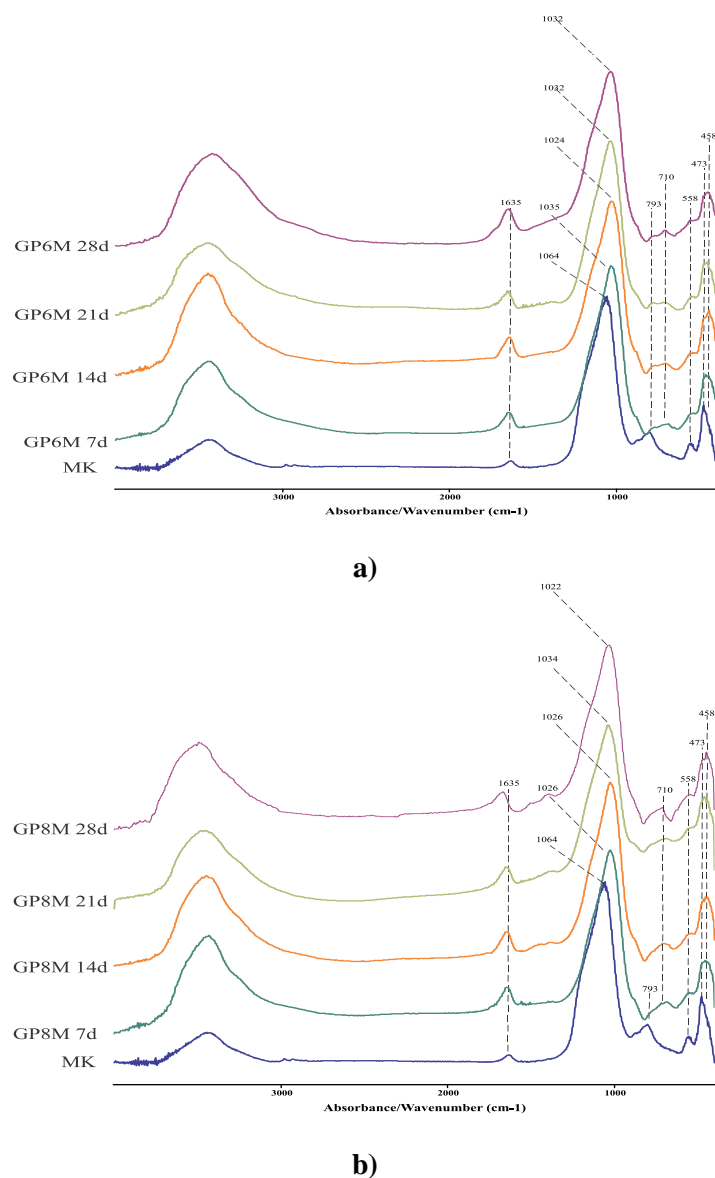


Fig. 3. FTIR of GP6M (a) and GP8M (b) sample after 7, 14, 21 and 28 days.

The FTIR Si–O, bending bands are detectable at 800 cm^{-1} and between 890 and 975 cm^{-1} . The band at approximately 1050 cm^{-1} is assigned to the Si–O stretching of tetrahedrons in which silicon is surrounded by 3 bridging oxygen units and one non-bridging oxygen (Si–NBO) [26, 27]. This structure is the building blocks of geopolymer of the Si–O–X (X = Al, Si, Na.). A shift of the Si–O–X stretching band towards lower wave numbers indicates lengthening Na, or H bond, reduction in the bond angle (230°) and this shift can be also attributed to an increase of the fraction of silicon sites with non-bridging oxygen atoms (NBO) [31]. In our case, the shift of the Si–O–X stretching band is evident. The wave number corresponding to the Si–O stretching for MK was detectable at 1064 cm^{-1} , for GP2M - 1044 cm^{-1} , for GP4M - 1036 cm^{-1} , for GP6M - 1032 cm^{-1} and GP8M - 1022 cm^{-1} after 28 days of aging.

The typical Al^{IV} absorption of the MK sample at around 800 cm^{-1} is not detectable in the geopolymer samples. However, there is peak at 710 cm^{-1} in the spectrum of the GP samples. According to the literature, in the $800\text{--}550\text{ cm}^{-1}$ region there are vibration bands attributed to Secondary Building Units (SBUs). SBUs are made of joined SiO_4 and AlO_4

tetrahedral forming variously membered rings [18, 29], which gives rise to an over-tetrahedral form of middle-range order. According to the literature [30], wide strip at 710cm^{-1} (of all geopolymer samples) could be attributed to asymmetric stretching Si-O-Al. On the other hand, the band of the Al-O bond at 793cm^{-1} is also shifted to the right. The intensity of the Si-O-Al (Si) bond band at 710cm^{-1} increases with concentration of NaOH. These shifts indicate that there are fine changes of the aluminosilicates structure as the geopolymer synthesis progresses. The intensity of the peaks at 558cm^{-1} for the GP6M and GP8M samples increases with the time. This type of addition has not been observed to samples GP2M and GP4M. Besides, the peak that occurs on MK at 473cm^{-1} is moving to the lower value of 458cm^{-1} for the GP6M and GP8M samples. Also, the bands at 793cm^{-1} and 458cm^{-1} could be assigned to quartz.

If we look at the end of the process (28th day) we can see clear influence of molarity. Peak that occurs on 1044cm^{-1} for sample GP2M is moving on 1022cm^{-1} for sample GP8M. It also shows a wide strip on 710cm^{-1} for GP8M sample, while on GP2M sample is not noticed. With increasing molarity of NaOH, intensity of strip on 793cm^{-1} is decreasing on the value of the strip on 710cm^{-1} .

Both methods XRD and FTIR, revealed that the concentration of NaOH has higher effect on structural changes in geopolymer than aging time.

3.1.3. MALDI-TOF analysis

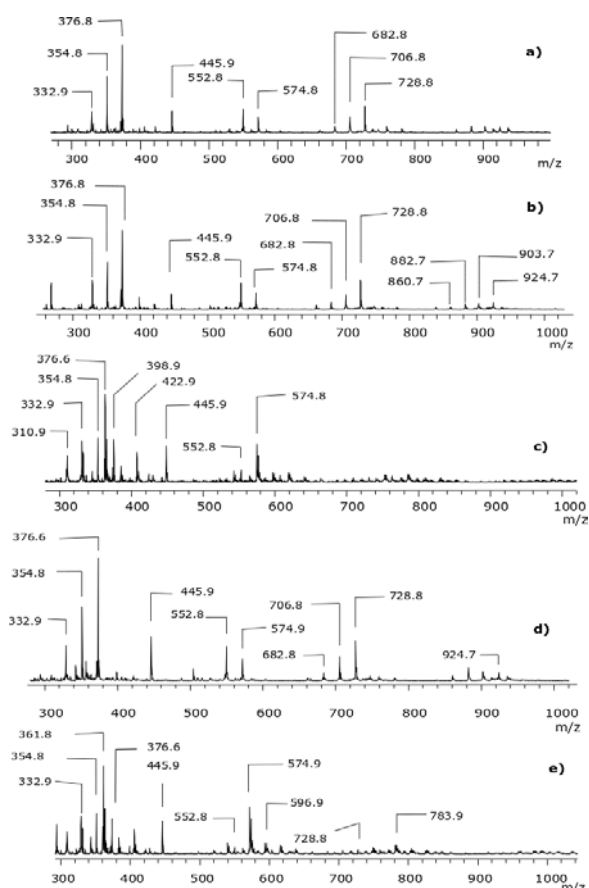


Fig. 4. Positive ion MALDI TOF mass spectra of metakaolin (a), and metakaolin treated with NaOH at varying concentrations, i.e. 2, 4, 6, 8 M (b,c,d,e and e, respectively).

Fig. 4 shows positive ion MALDI TOF mass spectra of metakaolin and metakaolin treated with NaOH at varying concentrations, 2, 4, 6, 8M. All detected signals in the spectra

fall in the m/z range below 1000, and the signals were compared with the spectrum of pure matrix. In general, singly positively charged ions arising from a geopolymer are generated either by addition of a proton from the molecule, or sodium when samples were treated with various concentrations of NaOH. All signals are basically formed from the fully protonated unit $\text{Al}_2\text{O}_3(\text{SiO}_2)_2$, with the addition of further SiO_2 unit, as well as the subsequent substitution of protons with sodium ions. Some signals were formed by the addition of a DHB molecule.

Signals with their position and identity are listed in Tab. III. The position is presented by mono isotopic mass of a singly positively charged ion.

The analysis of geopolymers by MALDI TOF MS is not a routine method, therefore, there are no corresponding literature data for comparison. In addition, the investigated system is highly alkaline, which affects the sensitivity of the detection, resulting in potentially suppressed signals at higher m/z ratios. Nevertheless, compared to non-treated MK, some new signals appear in the presence of NaOH, which are also at the higher m/z ratios, e.g. around m/z 900. Taken together, although no clear regularities could be established after MALDI mass spectrometric analysis, the spectra can provide the evidence of the effect that different concentrations of the NaOH in the activator solutions have on the structure of a geopolymer.

Tab. III Positions of signals detected in the spectra of geopolymers and their identity.

Position, m/z	Signal identity
310.88487	$\text{Al}_2\text{O}_3(\text{SiO}_2)_3\text{H}_6\text{Na}$
332.8668	$\text{Al}_2\text{O}_3(\text{SiO}_2)_3\text{H}_5\text{Na}_2$
354.84876	$\text{Al}_2\text{O}_3(\text{SiO}_2)_3\text{H}_4\text{Na}_3$
376.83071	$\text{Al}_2\text{O}_3(\text{SiO}_2)_3\text{H}_3\text{Na}_4$
422.89537	$\text{Al}_2\text{O}_3(\text{SiO}_2)_2\text{H}_4\text{Na}_3(\text{DHB}-2\text{H}+2\text{Na})$
445.88514	$\text{Al}_2\text{O}_3(\text{SiO}_2)_2\text{H}_3\text{Na}_4(\text{DHB}-2\text{H}+2\text{Na})$
552.8393	$\text{Al}_2\text{O}_3(\text{SiO}_2)_3\text{H}_3\text{Na}_4(\text{DHB}-\text{H}+\text{Na})$
574.82122	$\text{Al}_2\text{O}_3(\text{SiO}_2)_3\text{H}_3\text{Na}_4(\text{DHB}-2\text{H}+2\text{Na})$
682.79314	$\text{Al}_2\text{O}_3(\text{SiO}_2)_3(\text{AlSiO}_6\text{H}_4)\text{H}_5\text{Na}_2(\text{DHB}-3\text{H}+3\text{Na})$
706.79074	$\text{Al}_2\text{O}_3(\text{SiO}_2)_3(\text{AlSiO}_6\text{H}_4)\text{H}_4\text{Na}_3(\text{DHB}-3\text{H}+3\text{Na})$
728.77268	$\text{Al}_2\text{O}_3(\text{SiO}_2)_3(\text{AlSiO}_6\text{H}_4)\text{H}_3\text{Na}_4(\text{DHB}-3\text{H}+3\text{Na})$
860.74221	$\text{Al}_2\text{O}_3(\text{SiO}_2)_3(\text{AlSiO}_6\text{H}_4)_2\text{H}_3\text{Na}_4(\text{DHB}-\text{H}+\text{Na})$
882.72416	$\text{Al}_2\text{O}_3(\text{SiO}_2)_3(\text{AlSiO}_6\text{H}_4)_2\text{H}_2\text{Na}_5(\text{DHB}-\text{H}+\text{Na})$
903.69882	$\text{Al}_2\text{O}_3(\text{SiO}_2)_3(\text{AlSiO}_6\text{H}_4)_2\text{H}_1\text{Na}_6(\text{DHB}-\text{H}+\text{Na})$
924.6724	$\text{Al}_2\text{O}_3(\text{SiO}_2)_3(\text{AlSiO}_6\text{H}_4)_2\text{H}_3\text{Na}_7(\text{DHB}-\text{H}+\text{Na})$

3.2. Morphological analysis

As a final step, we have performed the SEM analyses in order to identify the reactants of metakaolin according to the alkaline activator and to verify the internal microstructure. This study focused on analyzing the microstructure of the geopolymer formed after 28 days of curing or aging. The species of different types of morphologies formed during the geopolymerization process.

The surfaces of the geopolymers GP2M, GP4M, GP6M and GP8M aging for 28 days are shown in fig. 5 a-d. Sodium hydroxide alkaline activator dissolved metakaolin particle, and that process results in the inorganic polymer gel phase formation [31]. The microstructures of the samples obtained using different concentration of NaOH are different. Fig. 5a shows micrographs of GP2M. We see the foam structure, probably incomplete process dissolving of metakaolin and incomplete geopolymerization. It is evident that the structure of GP2M is loosened, compared to other samples. Fig. 5b shows numbered individual particles,

aggregates as well as the appearance of the gel phase, and the formation of the sticks, or plates of GP4M sample. The structure of GP6M is compact with the appearance of a small number of individual particles or a group of particles. GP8M layered gel porous structure is shown on the Fig. 5d. There are also a certain number of single particles. The samples show a porous microstructure formed by unreacted micron size particles and a geopolymeric matrix that is formed during the polycondensation. Based on the Fig.s, we can see that with increasing NaOH, the newly formed sample contains part of the sample structure with a lower concentration of NaOH, and that the second part of the sample are newly formed structure. The microstructures of GP2M, GP4M and GP6M (Fig. 5a, b, c) show intergranular cracks that indicate that the interfaces in these investigated geopolymer samples are weak. Determination of static water contact angle makes to define hydrophobicity of samples and possible surface modifier in terms of the type of applications of geopolymers [32]. GP8M (Fig. 5d) after 28 days of aging shows that the microstructure consists of dense plates formed by the geopolymerization of metakaolin. However, the geopolymer dense plates that are observed indicate that these are the strongest constituents.

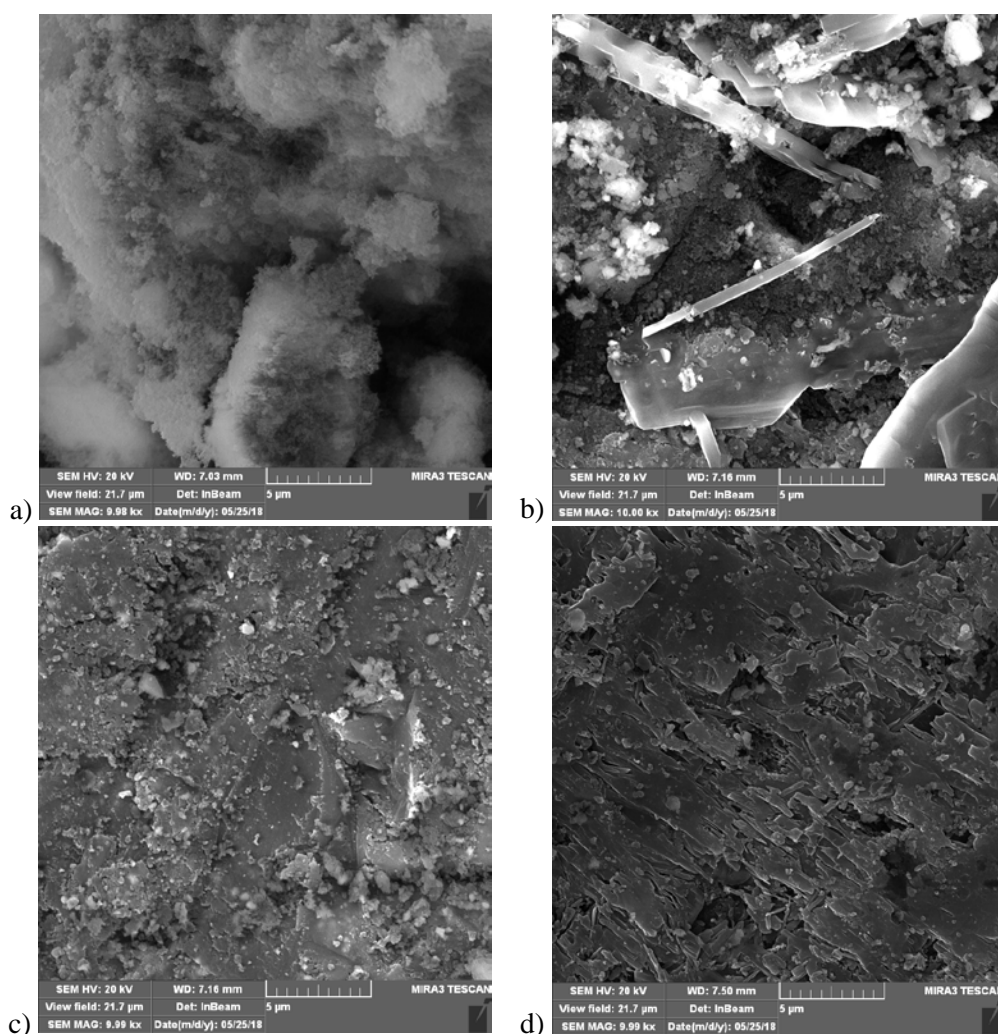


Fig. 5. SEM of GP2M (a), GP4M (b), GP6M (c) and GP8M (d).

4. Conclusion

Results presented in this paper reveal a diverse influence that the concentration of NaOH and aging time have on a process of polymerization of a metakaolin. More compact structure of the geopolymer, which correlates to the degree of polymerization is obtained with increasing concentration of NaOH, but also with the time of aging. On the other hand, no significant changes in its crystallinity have been observed with the increase of NaOH concentration in the activation solution. The most important outcome of this study is that is possible to control the properties of a geopolymer, with respect to its application, by avoiding the investment of the energy and solely by the process that is completely eco-friendly.

5. References

1. P. Duxson, A. Fernández-Jiménez, L. Provis, G. C. Lukey, A. Palomo, J. S. J. van Deventer, *J. Mater. Sci.*, 42(9) (2007)2917-2933
2. G. Habert, J.B. de d'EspinoseLacaille and N. Roussel, *J. Clean. Product.*, 19 (11) (2011) 1229-1238.
3. K. Komnitsas, I. Kourti, S. Onisei, Y. Pontikes, C. Cheeseman, P. Moldovan, A. Boccaccini, in: 2nd International Slag Valorisation Symposium, Leuven, Belgium, 2011, Proceedings pp. 63-78.
4. J.L. Provis, P. Duxson and J.S.J.vanDeventer, *Adv. Powder Technol.*, 21(1)(2010) 2-7.
5. Y. Wu, B. Lu, T. Bai, H. Wang, F. Du, Y. Zhang, L. Cai, C. Jiang, W. Wang, Geopolymer, green alkali activated cementitious material: Synthesis, applications and challenges, *Construction and Building Materials* Volume 224, 2019, 930-949
6. P. De Silva, K. Sago-Crenstil, V. Sirivivatnanon, *Cement Concrete Res.*, 37 (2007) 512-518.
7. H. Wang, H. Li, F. Yan, Synthesis and mechanical properties of metakaolinite- based geopolymer, *Colloids and Surfaces A: Physicochem. Eng. Aspects* 268 (2005) 1-6.
8. S. Alonso, A. Palomo, *Materials Letters*, 2(47) (2001) 55-62.
9. J.G.S Jaarsveld, J.S.J. Deventer, G.C. Lukey, *Chem. Eng. J.*, 89(2002) 63-73.
10. B.V. Rangan, Fly ash-based geopolymer concrete, Research report GC4, Engineering Faculty, Curtin University of Technology, Perth, Australia.
11. K. Trivunac, Lj. Kljajević, S. Nenadović, J. Gulicovski, M. Mirković, B. Babić, S. Stevanović, *Sci. Sinter.*, 48 (2016) 209-220.
12. S. Nenadović, Lj. Kljajević, M. Nešić, M. Petković, K. Trivunac, V. Pavlović, *Environ. Earth. Sci.*, (2017) 76-79.
13. Rigaku Corporation, Tokyo J. PDXL Version 2.8.3.0 Integrated X-ray Powder Diffraction Software. 2011.
14. Powder Diffraction File P-D, announcement of new data-base release 2012, International Centre for Diffraction Data (ICDD)
15. D.M. Gonzales-Garcia, L. Tellez-Jurado, F.J. Jimenez-Alvarez, H. Balmori-Ramirez, *Ceram. Inter.*, 43 (2017) 2606-2613.
16. A.M. Mustafa Al Bakri, H. Kamarudin, M. Bnhussain, I. KhairulNizar, A.R. Rafiza & A.M. Izzat, Chemical Reactions in the Geopolymerisation Process Using Fly Ash-Based Geopolymer: A Review, *Australian Journal of Basic and Applied Sciences*, 5(7) (2011)1199-1203.
17. B. Zhang, K. J. D. MacKenzie, I. W. M. Brown, Crystalline phase formation in metakaolinitegeopolymers activated with NaOH and sodium silicate, *J Mater Sci* (2009) 44, 4668-4676.
18. N. Lee, H.R. Khalid, H. Lee, *Microporous Mesoporous Mater.*, 229 (2016) 22-30.
19. J.L. Provis, G.C. Lukey, J.S. van Deventer, *Chem. Mater.*, 17 (2005) 3075 3085.
20. A. Palomo, F. Glasser, *Br. Ceram. Trans.*, J. 91 (1992) 107-112.

21. P. Rožek, M. Król, W. Mozgawa, Geopolymer-zeolite composites: A review, Journal of Cleaner Production 230 (2019) 557-579.
22. Lj. Kljajević, S. Nenadović, M. Nenadović, N. Bundaleski, B. Todorović, V. Pavlović and Z. Rakočević, Ceram. Inter., 43 (9) (2017) 6700-6708.
23. L. Verdolotti, S. Iannace, M. Lavorgna, R. Lamanna, J. Mater. Sci., 43 (2008) 865-873.
24. E. Prud'homme, P. Michaud, E. Joussein, A. Smith, C. Peyratout, I. Sobrados, J. Sanz, S. Rossignol, J. Sol-Gel Sci. Technol., 61 (2012) 436-448.
25. M.E. Simonsen, C. Sonderby, Z. Li, E.G. Sogaard, J. Mater. Sci., 44(2009) 2079-2088.
26. C. Karlsson, E. Zanghellini, J. Swenson, B. Roling, D.T. Bowron, L. Börjesson, Phys. Rev. B, 72 (2005) 064206.
27. P. Innocenzi, J. Non Cryst. Solids, 316 (2003)309-319.
28. A. Fernandez-Jimenez, A. Palomo, MicroporousMesoporous Mater., 86 (2005) 207-214.
29. M. Alkan, C. Hopa, Z. Yilmaz, H. Guler, MicroporousMesoporous Mater., 86 (2005) 176-184.
30. A. Allahverdi, K. Mehrpour & E. N. Kani, IUST International Journal of Engineering Science,19 (3)(2008)1-5.
31. Z Zhang, Hao Wang, John L. Provis, Frank Bullen, Andrew Reid, Yingcan Zhu, Quantitative kinetic and structural analysis of geopolymers. Part1. The activation of metakaolin with sodium hydroxide, Thermochemica Acta 539 (2012) 23-33.
32. Lj. M. Kljajević, Z. Melichova, D. D. Kisić, M. T. Nenadović, B. Ž. Todorović, V. B. Pavlović, S. S. Nenadović, Sci. Sinter., 51(2019) 163-173.

Сажетак: У раду је приказано добијање неорганског полимера/геополимера на бази метакаолина, еколошки чистом технологијом уз уштеду енергије да би се очувла природна средина и ресурси. Испитан је утицај алкалне активације, односно различите концентрације NaOH као компоненте смеше алкалног активатора, на процес геополимеризације метакаолина. Такође, коришћењем неколико аналитичких метода праћен је процес старења геополимера. Структура метакаолина и геополимера заснованих на метакаолину и њихова физичко-хемијска својства проучаван су рендгенском дифракцијом (XRD), инфрацрвеном спектроскопијом са Фуријеовом трансформацијом (FTIR), а након 28 дана примењена је скенирајућа електронска микроскопија (SEM) са енергетско дисперзионом спектроскопијом (EDS) за карактеризацију површине узорака. FTIR је регистовао померање Si-O или Si-O-X (X = Al, Si, Na ...) веза са повећањем моларитета алкалног активатора током процеса геополимеризације. Масени спектар геополимера је окарактерисан MALDI TOF масеним спектрометром. Током очвршћавања/старења дошло је до структурне реорганизације узорака геополимера у складу са механизмом геополимеризације.

Кључне речи: метакаолин, алкална активација, неоргански полимер, време старења, MALDI TOF MS.

